

2018

Detection of Bisphenol A and Derivatives in Human Urine via Cyclodextrin-Promoted Fluorescence Modulation

Dana J. DiScenza
University of Rhode Island

Julie Lynch
University of Rhode Island

Ezra Feder
University of Rhode Island

Mindy Levine
University of Rhode Island, m_levine@uri.edu

Follow this and additional works at: https://digitalcommons.uri.edu/chm_facpubs

Citation/Publisher Attribution

DiScenza, D. J., Lynch, J., Feder, E., & Levine, M. (2018). Detection of Bisphenol A and Derivatives in Human Urine via Cyclodextrin-Promoted Fluorescence Modulation. *Anal. Methods*, *10*, 3783-3790. doi: 10.1039/C8AY00733K
Available at: <http://dx.doi.org/10.1039/C8AY00733K>

This Article is brought to you by the University of Rhode Island. It has been accepted for inclusion in Chemistry Faculty Publications by an authorized administrator of DigitalCommons@URI. For more information, please contact digitalcommons-group@uri.edu. For permission to reuse copyrighted content, contact the author directly.

Detection of Bisphenol A and Derivatives in Human Urine via Cyclodextrin-Promoted Fluorescence Modulation

The University of Rhode Island Faculty have made this article openly available.
Please let us know how Open Access to this research benefits you.

This is a pre-publication author manuscript of the final, published article.

Terms of Use

This article is made available under the terms and conditions applicable towards Open Access Policy Articles, as set forth in our [Terms of Use](#).



Detection of Bisphenol A and Derivatives in Human Urine via Cyclodextrin-Promoted Fluorescence Modulation

Dana J. DiScenza,^a Julie Lynch,^a Ezra Feder,^a and Mindy Levine^{*a}

Received 00th January 20xx,
Accepted 00th January 20xx

DOI: 10.1039/x0xx00000x

www.rsc.org/

Reported herein is the sensitive and selective detection of bisphenol A (BPA) and six BPA derivatives in buffer and urine environments. This detection system relies on the ability of γ -cyclodextrin to act as a supramolecular scaffold to promote highly analyte-specific, proximity-induced fluorescence modulation of high quantum yield fluorophores, which led to unique modulation responses for each cyclodextrin-analyte-fluorophore combination investigated in both buffer and urine environments, and high selectivity between structurally similar analytes using linear discriminant analysis of the resulting response signals. This method was sensitive (low micromolar detection limits), selective (able to differentiate between structurally similar analytes), and broadly applicable (with successful detection in both buffer and urine environments), and has significant potential in the detection of BPA and its derivatives in a wide variety of complex environments.

Introduction

Among the list of known and suspected environmental toxicants, bisphenol A (BPA) and its derivatives,¹ including bisphenol S (BPS) and bisphenol F (BPF),² have received a significant amount of attention in both the scientific literature³ and the popular media. BPA is a suspected endocrine disruptor,⁴ and exposure to BPA and associated derivatives is correlated with increased rates of asthma,⁵ inflammatory bowel disease,⁶ endocrine disorders,⁷ and certain cancer sub-types.⁸ These negative health effects are particularly concerning because of BPA's ubiquitous presence in a variety of commercial products, including plastic water bottles⁹ and bags,¹⁰ liners of canned food products,¹¹ infant bottles¹² and training (*i.e.* "sippy") cups,¹³ and cash register receipts.¹⁴

As a result of these deleterious health effects, many regulatory agencies have banned the use of BPA in commercial products.¹⁵ Manufacturers have replaced BPA with a variety of alternatives;¹⁶ however, the use of BPA-like derivatives are particularly concerning due to the limited amount of toxicity data associated with these compounds,¹⁷ and the fact that available data suggests that BPA derivatives can be even more toxic than BPA itself.¹⁸

There are almost no regulations associated with the use of BPA derivatives to date, nor are there any detailed regulations about the use of the label "BPA-free" on commercial products, which means that products that are labelled as "BPA-free" may contain significant amounts of BPA and BPA derivatives.¹⁹ One biological fluid that is particularly important for the detection of BPA and BPA derivatives

is human urine, due to the non-invasive sample collection procedures and the relative simplicity of the matrix compared to other biological fluids.²⁰ BPA and its derivatives have been found in the urine of about 90% of the U.S. population.²¹ The relative dearth of regulations around BPA labelling,²² combined with the known and suspected deleterious health effects of BPA exposure,²³ and prevalence of BPA and its derivatives in human urine, means that methods for BPA detection that are sensitive, selective, rapid, and practical for real-world usage are sorely needed.

Reported methods for the detection of BPA and BPA derivatives focus predominantly on the use of mass spectrometry based methods, including gas chromatography-mass spectrometry (GC-MS)²⁴ and high-pressure liquid chromatography (HPLC)²⁵ with mass spectrometry detection.²⁶ While these methods provide exquisite sensitivity for even trace amounts of BPA, their use comes with significant drawbacks in terms of the cost associated with such methods, the level of expertise required to operate this instrumentation, and the time required to achieve high levels of purification that enable such sensitive detection. Newer methods, including electrochemical assays,²⁷ colorimetric detection,²⁸ and Raman spectroscopy-based methods,²⁹ have also been reported.

Previous work in our group has focused on the detection of a variety of aromatic and non-aromatic toxicants, using cyclodextrin-promoted energy transfer³⁰ (for photophysically active toxicants) and cyclodextrin-promoted fluorescence modulation (for non-photophysically active analytes) (Fig. 1).³¹

^a Department of Chemistry, University of Rhode Island, 140 Flagg Road, Kingston, RI 02881; mindy.levine@gmail.com; 401-874-4243

Electronic Supplementary Information (ESI) available: Details of analytes and fluorophores, summary tables and summary figures for fluorescence modulation, limit of detection, array generation, GC-MS characterization, mixture fluorescence modulation, mixture array generation, and binding constant experiments. See DOI: 10.1039/x0xx00000x

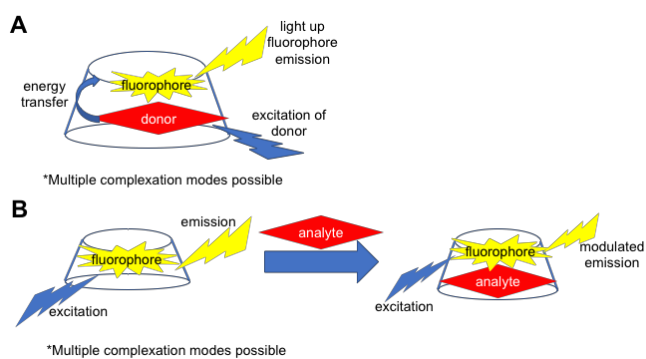


Fig. 1 Schematic of cyclodextrin-promoted (A) energy transfer and (B) fluorescence modulation

We demonstrated that this toxicant detection system operates in a broad range of environments, including plasma,³² breast milk,³³ and urine,³⁴ as well as in extracts collected in the aftermath of the 2010 Deepwater Horizon oil spill.³⁵ Although our previous work detected polycyclic aromatic hydrocarbons,³⁶ polychlorinated biphenyls,³⁷ aromatic amines, pesticides,³⁸ aliphatic alcohols, and fuel spill components, we have not used cyclodextrin systems for the detection of BPA and BPA derivatives to date.

Reported herein is the rapid, sensitive, and selective detection of BPA and BPA derivatives in buffer and urine environments using cyclodextrin-promoted fluorescence modulation. This detection system uses commercially-available cyclodextrin hosts and fluorophore dyes to facilitate such detection. This method operates with high sensitivity (low micromolar detection limits), high selectivity (100% differentiation between structurally similar analytes), and general applicability (100% differentiation between binary mixtures of structurally similar analytes).

Experimental

Instruments and Reagents

All analytes and fluorophores (compounds **1-11**, Fig. 2) were purchased from Sigma-Aldrich Chemical Company and used as received, unless otherwise noted. γ -Cyclodextrin was purchased from Tokyo Chemical Industry and used as received. UV-Visible spectra were obtained using an Agilent 8453 UV/Visible spectrometer. Fluorescence spectra were obtained using a Shimadzu RF-5301PC spectrofluorimeter with 1.5 nm excitation and emission slit widths. All GC-MS measurements were obtained using a Shimadzu GC-MS QP2020 gas chromatograph-mass spectrometer. Urine was obtained from a single anonymous human donor and stored in amber high-density polyethylene bottles in the refrigerator until use. Computational experiments were performed using Spartan 16 software. Arrays were generated using SYSTAT 13 statistical computing software.

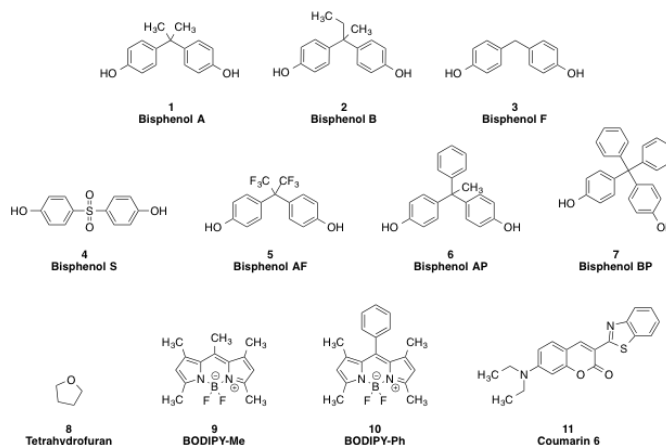


Fig. 2 Structures of analytes **1-7**, control analyte **8**, and fluorophores **9-11**

General Procedure for GC-MS Characterization Experiments

GC-MS sample preparation was conducted following literature-reported procedures.³⁹ Approximately 10 mL of the urine sample was added to a separatory funnel. Then, 15 mL of dichloromethane was added to the separatory funnel, and the separatory funnel was shaken vigorously. The organic layer was collected, and another 15 mL of dichloromethane was added to the urine layer. The organic layer was collected, another 15 mL of dichloromethane was added to the urine, and the procedure was repeated. The remaining organic layer was dried with MgSO_4 , filtered, concentrated to 1 mL using a rotary evaporator, and analysed by GC-MS.

All GC-MS measurements were obtained on a Shimadzu QP2020 gas chromatograph-mass spectrometer with the following settings: column: Shimadzu SH-Rxi-5SiIMS (30 m x 0.25 mm x 0.25 μm); oven temperature: 45 $^\circ\text{C}$, hold for 7 min, ramp to 200 $^\circ\text{C}$ at 20 $^\circ\text{C}/\text{min}$, hold for 60 min; injection temperature: 200 $^\circ\text{C}$; splitting ratio: splitless; MS ion source temperature: 230 $^\circ\text{C}$; interface temperature: 150 $^\circ\text{C}$; total run time: 75 min.

General Procedure for Fluorescence Modulation Experiments

In a quartz cuvette, 1.25 mL of a 10 mM γ -cyclodextrin solution dissolved in phosphate buffered saline (PBS) and 1.25 mL of a urine sample were combined and mixed thoroughly. For control experiments in the absence of urine, 2.5 mL of a γ -cyclodextrin solution was used. Next, 100 μL of a 0.1 mg/mL fluorophore solution in tetrahydrofuran (THF) was added, and the solution was excited four times at the excitation wavelength of the fluorophore (460 nm for fluorophores **9** and **10** and 420 nm for fluorophore **11**). Then, 50 μL of analytes **1-8** (1.0 mg/mL solution in THF) were added to the mixture, and the resulting solution was excited four times at the excitation wavelength of the fluorophore. The fluorescence emission spectra were integrated vs. wavenumber on the X-axis using OriginPro software, and the fluorescence modulation was measured by the ratio of the integrated emission of the fluorophore in the presence of the analyte to integrated emission of the fluorophore in the absence of the analyte, as shown in Equation 1:

$$\text{Fluorescence modulation} = F_{\text{analyte}}/F_{\text{blank}} \quad (\text{Eq. 1})$$

Where $F_{analyte}$ is the integrated fluorescence emission of the fluorophore in the presence of analyte, and F_{blank} is the integrated fluorescence emission of the fluorophore in the absence of the analyte. Fluorescence modulation ratios greater than 1 indicate an enhancement of fluorescence emission of the fluorophore in the presence of analyte, fluorescence modulation ratios less than 1 indicate a decrease in fluorescence emission of the fluorophore in the presence of analyte, and fluorescence modulation ratios close to 1 indicate minimal change in fluorescence emission of the fluorophore in the presence of analyte.

General Procedure for Limit of Detection Calculations

The limit of detection (LOD) is defined as the lowest concentration of analyte at which a signal can be detected. To determine this value, the following steps were performed for each water-cyclodextrin-analyte combination.⁴⁰ In a quartz cuvette, 1.25 mL of 10 mM γ -cyclodextrin in PBS and 1.25 mL of urine sample were combined. In the absence of urine, 2.5 mL of γ -cyclodextrin solution was used. Then, 100 μ L of a fluorophore **9** (0.1 mg/mL solution in THF) was added, the solution was excited at 460 nm, and the fluorescence emission spectra were recorded. Six measurements were taken.

Next, 20 μ L of analyte (1.0 mg/mL in THF) were doped into an aqueous sample, and again the solution was excited at the fluorophore's excitation wavelength, and the fluorescence emission spectra were recorded. Six repeat measurements were taken. This step was repeated for 40 μ L of analyte, 60 μ L of analyte, 80 μ L of analyte, and 100 μ L of analyte, all of which were doped into a urine sample that did not initially contain toxicants, to measure the ability of the system to detect the doped toxicants within the complex aqueous matrix.

All of the fluorescence emission spectra were integrated vs. wavenumber on the X-axis using OriginPro software, and calibration curves were generated. The curves were plotted with the analyte concentration in μ M on the X-axis, and the fluorescence modulation ratio on the Y-axis. The curve was fitted to a straight line and the equation of the line was determined (see ESI for full details). The limit of detection was calculated according to Equation 2:

$$\text{LOD} = 3(\text{SD}_{\text{blank}})/m \quad (\text{Eq. 2})$$

Where SD_{blank} is the standard deviation of the blank, analyte-free sample and m is the slope of the calibration curve. All LODs were reported in μ M.

General Procedure for Array Generation Experiments

Array analysis was performed using SYSTAT 13 statistical computing software with the following settings: (a) Classical discriminant analysis; (b) Grouping variable: analytes; (c) Predictors: fluorophores; and (d) Long-range statistics: Mahal

General Procedure for Binding Constant Experiments

In a quartz cuvette, 2.5 mL of PBS and 50-100 μ M of analyte were combined and mixed thoroughly. The absorbance of the sample was measured across the full UV and visible range. This procedure was

repeated for 5.00×10^{-6} M, 1.00×10^{-5} M, 5.00×10^{-5} M, 1.00×10^{-4} M, 5.00×10^{-4} M, 1.00×10^{-3} M, 1.50×10^{-3} M, and 2.50×10^{-3} M γ -cyclodextrin in PBS with constant analyte concentration (see ESI for full details). Double reciprocal Benesi-Hildebrand plots were generated following literature-reported procedures.⁴¹ Binding constants were calculated using Equation 3:

$$1/\Delta A = 1/b\Delta\epsilon[G][H]_0K_a + 1/b\Delta\epsilon[H]_0 \quad (\text{Eq. 3})$$

Where A is the change in absorbance, specifically the absorbance of analyte in the presence of cyclodextrin minus the absorbance of analyte in the blank, cyclodextrin-free sample in absorbance units, b is the path length of 1 cm, $\Delta\epsilon$ is the change in the absorption coefficient of the analyte-cyclodextrin complex minus the absorption coefficient of the analyte in cyclodextrin-free solution in $\text{L}\cdot\text{cm}^{-1}\cdot\text{mol}^{-1}$, $[G]$ is the cyclodextrin concentration in molar (M), $[H]_0$ is the analyte concentration, and K_a is the binding constant in M^{-1} .

Results and discussion

Urine Characterization

GC-MS was used to characterize the analyte-free urine sample (Fig. 3).

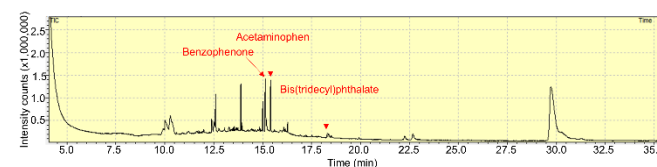


Fig. 3 GC-MS spectrum of human urine sample

The undoped urine sample showed peaks that corresponded to long-chain alkanes, fatty acids, and amides, all of which are commonly found in urine.⁴² Notably, the urine sample also contained GC-MS peaks that corresponded to benzophenone,⁴³ commonly used in personal care products such as sunscreen⁴⁴ and lip balm,⁴⁵ phthalates, commonly found in plastics⁴⁶ and some food products,⁴⁷ and acetaminophen, commonly found in over-the-counter pain relievers.⁴⁸

Selection of Fluorophores

Previous work in our group focused on the use of a BODIPY fluorophore with a free thiol moiety, which was synthesized in several steps. In order to develop more practically applicable detection systems, this work uses commercially available BODIPY compounds (fluorophores **9** and **10**), as well as coumarin **6** (fluorophore **11**), which is commercially available, and has high quantum yields and excellent aqueous stability.

Selection of Cyclodextrins

Previous work in our group has used of a variety of commercially available cyclodextrins: α -cyclodextrin, β -cyclodextrin, randomly methylated β -cyclodextrin (with an average of 1.8 methyl groups per unit),⁴⁹ 2-hydroxypropyl- β -cyclodextrin, and γ -cyclodextrin, for cyclodextrin-promoted energy transfer and fluorescence modulation.

Table 1 Calculated properties of analytes and fluorophores

Compound	Area ^a (Å ²)	Solvent-accessible surface area ^a (Å ²)	Volume ^a (Å ³)	Binding in γ -cyclodextrin ^b (M ⁻¹)	Electrostatic potential ^c (min/max) (kJ mol ⁻¹)
1	245	179	246	3.22 x 10 ⁴	-141/273
2	259	184	265	2.37 x 10 ⁴	-139/273
3	220	171	210	1.39 x 10 ⁴	-139/273
4	233	179	225	1.79 x 10 ⁴	-200/313
5	260	178	261	7.83 x 10 ⁴	-122/295
6	295	214	307	5.99 x 10 ⁴	-139/275
7	344	254	367	1.06 x 10 ⁵	-140/275
8	104	84	86.3	^c	-139/68.2
9 ^d	262	194	266	5.33 x 10 ³	-231/121
10 ^d	313	221	329	^c	-229/127
11 ^d	344	261	349	1.75 x 10 ⁴	-202/118

^aValues were calculated using Spartan 16 software. ^bBinding constants calculated by UV/Visible spectroscopy (see ESI for more details). ^cNo binding constant value was obtained. ^dBinding constants measured by fluorescence spectroscopy.

Table 2 Literature-reported dimensions of γ -cyclodextrin^a

Compound	Outer diameter (Å)	Cavity diameter (Å)	Height of torus (Å)	Cavity volume (Å ³)
γ -cyclodextrin	17.5	7.5-8.3	7.9	427

^aValues were obtained from the literature⁵⁰

Due to the relatively large size of the analytes and the fluorophores in this system, γ -cyclodextrin was selected (Table 1 and Table 2). Of note, increases in the fluorophore emission intensity were observed in the presence of γ -cyclodextrin compared to in cyclodextrin-free solution, even in the absence of any added analyte (see ESI for more details). These increases can be attributed to the fact that binding in the cyclodextrin cavity decreases non-radiative decay pathways for the fluorophores and increases the resultant quantum yield, a phenomenon which has been observed previously.⁵¹

Fluorescence Modulation

Fluorescence modulation experiments measure the ability of a particular analyte to induce measurable, analyte-specific changes in the fluorescence emission spectra of a high quantum yield fluorophore. Micromolar concentrations of analytes **1-7** or control analyte **8** were added to each cyclodextrin-fluorophore combination or urine-cyclodextrin-fluorophore combination. The degree of fluorescence modulation of fluorophores **9-11** in the presence of and absence of analyte was calculated using Eq. 1.

Based on computational results, it is evident that both the analyte and fluorophore do not bind in the cyclodextrin cavity together due to lack of available space (Table 1, Table 2). Nonetheless, the addition of analyte promotes binding of the fluorophore, via mechanisms that

Table 3 Fluorescence modulation values for analytes **1-8** with fluorophore **9**^a

Analyte	Buffer	Urine
1	1.19 ± 0.01	1.36 ± 0.02
2	1.20 ± 0.00	1.36 ± 0.02
3	1.68 ± 0.01	1.85 ± 0.01
4	1.19 ± 0.00	1.34 ± 0.01
5	1.18 ± 0.00	1.38 ± 0.01
6	1.19 ± 0.01	1.39 ± 0.01
7	1.18 ± 0.01	1.36 ± 0.01
8	1.17 ± 0.01	1.32 ± 0.00

^aAll results represent an average of results from four trials for each sample. Fluorescence modulation values were calculated using Eq. 1.

we are still investigating, leading to subsequent increases in fluorescence emission of the fluorophore. It is important to note that while experimental conditions (i.e. temperature, pH, solvent, etc.) have an effect on the fluorescence modulation response in general,⁵² our system controls these particular experimental parameters both before and after analyte addition so that they remain consistent..

Specifically in the case of fluorophore **9**, the fluorescence modulation values were greater than 1, indicating that introduction of analytes **1-7** and control analyte **8** led to an increase in the fluorescence emission of fluorophore **9** (Table 3). In this three-component system (analyte, fluorophore **9**, and cyclodextrin), the effect of analyte addition is to promote binding of the fluorophore inside the cyclodextrin cavity, resulting in the observed fluorescence increases.

Of note, the fluorescence modulation values in urine were uniformly higher than the values obtained in buffer, meaning that analyte addition in urine caused a larger increase in fluorescence compared to the fluorescence increases in buffer (see ESI for more details). Known differences in the composition of urine compared to buffer include higher concentrations of electrolytes as well as a lower pH value. For both factors, the net result is an increase in the concentration of charged species in solution, which can cause salt-induced increases in key intermolecular interactions, including hydrophobic association and intermolecular hydrogen bonding, following literature precedent.⁵³

In comparing the fluorescence modulation values of different analytes, many of the analytes induce similar fluorescence changes, which again can be attributed to their ability to promote binding of the fluorophore **9** in the cyclodextrin cavity (Fig. 4).

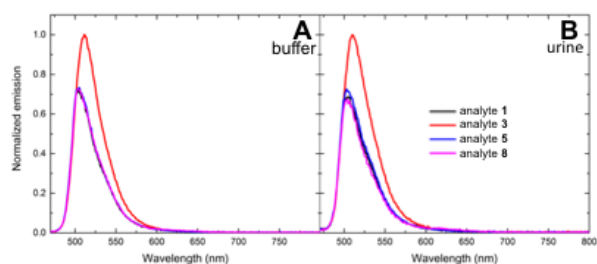


Fig. 4 Fluorescence changes of fluorophore **9** ($\lambda_{\text{ex}} = 460$ nm) in (A) buffer and (B) urine with analytes **1**, **3**, **5**, and **8**. The black line represents analyte **1**, the red line represents analyte **3**, the blue line represents analyte **5**, and the purple line represents analyte **8**.

Table 4 Fluorescence modulation values for analytes **1-8** with fluorophore **10**^a

Analyte	Buffer	Urine
1	1.03 ± 0.00	1.03 ± 0.00
2	0.86 ± 0.01	0.95 ± 0.00
3	0.68 ± 0.01	0.92 ± 0.01
4	0.84 ± 0.00	0.92 ± 0.01
5	0.83 ± 0.00	0.94 ± 0.01
6	0.84 ± 0.01	0.99 ± 0.01
7	0.81 ± 0.01	0.90 ± 0.00
8	1.03 ± 0.01	1.09 ± 0.01

^aAll results represent an average of results from four trials for each sample. Fluorescence modulation values were calculated using Eq. 1.

Particularly high modulation values were observed for bisphenol F (analyte **3**), which is the only analyte that has no substitution at the methylene position. This structural anomaly, in turn, likely means that it has less steric hindrance and dimensions that enable it to bind in or associate close to the γ -cyclodextrin cavity with fluorophore **9**. (Table 1, Table 2, Fig. 5). In contrast, the substitution of the methylene position with other analytes means that such ternary complex formation is less favored, and that other differences in substitution patterns (analyte **1** vs analyte **5**, for example) lead to minimal differences in the modulation values.

In most cases, the fluorescence modulation values for fluorophore **10** were less than 1, indicating that introduction of analytes **1-7** and control analyte **8** led to a decrease in the fluorescence emission of fluorophore **10** (Table 4). The responses for fluorophore **10** indicated the presence of a fluorophore excimer peak (Fig. 6), as a result of the binding of two molecules of fluorophore **10** in the γ -cyclodextrin cavity. In such cases, introduction of the bisphenol analyte leads to the replacement of one of the two fluorophores from the cavity, leading to a decrease in the excimer emission and fluorescence modulation responses lower than 1.

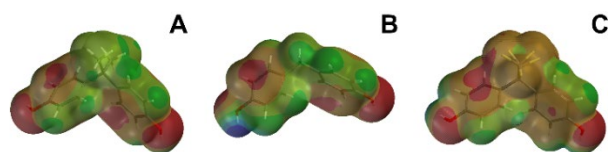


Fig. 5 Electrostatic potential maps of (A) analyte **1**, (B) analyte **3**, and (C) analyte **5**. All surfaces were generated using energy minimized geometries.

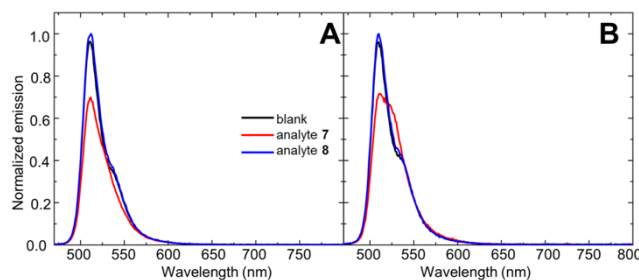


Fig. 6 Fluorescence changes of fluorophore **10** ($\lambda_{\text{ex}} = 460$ nm) in (A) buffer and (B) urine with analytes **7** and **8**. The black line represents no analyte, the red line represents analyte **7**, and the blue line represents analyte **8**.

In every case, the fluorescence modulation values for fluorophore **11** were greater than 1, indicating that introduction of analytes **1-7** and control analyte **8** led to an increase in the fluorescence emission of fluorophore **11** (Table 5). These increases were generally lower in the magnitude that the increases observed for fluorophore **9**, indicating that the analyte-induced changes in the binding of fluorophore **11** in the cavity were lower than those of fluorophores **9** and **10**. Additionally, the signal-to-noise ratio of all spectra containing fluorophore **11** is lower than spectra obtained in the presence of fluorophores **9** and **10**. This different behaviour is likely a result of the fact that fluorophores **9** and **10** have higher quantum yields compared to fluorophore **11**,⁵⁴ and that as a result of both of these features, binding of fluorophore **11** in the γ -cyclodextrin cavity is more highly favoured. In support of this statement, electrostatic potential mapping of fluorophore **11** and fluorophores **9** and **10** show marked differences, both in terms of variation in electrostatic potential as well as in overall size and shape of the fluorophore (Fig. 7). These marked differences in the electrostatic potentials as well as solvent accessible surface areas (Table 1) contribute to the differences in interactions for each cyclodextrin-fluorophore-analyte combination. Fluorophore **11** has a number of advantages in terms of detection applications (high quantum yield, aqueous stability, etc), and our group has used it previously for a variety of turn-on detection schemes. The differential performance of fluorophores **9** and **10** compared to fluorophore **11** in this context provides important information for the array-based selectivity.

Array Generation

The selectivity of this system for structurally similar bisphenol derivatives was determined using array-based analysis of the fluorescence response patterns. This analysis resulted in 100% differentiation between analytes in both purified buffer and urine (Fig. 8A and 8C). The response patterns are markedly distinct for buffer and urine environments, and show unique, well-separated signals for structurally similar bisphenols within each sample. The high degree of success and noticeable visual differences between environments highlight the power of this statistical method in distinguishing even very slight structural differences (analytes **1** and **2**, analytes **1** and **5**, and analytes **6** and **7**). Given the high degree of

fluorescence modulation of fluorophores **9** and **10** and slight change of fluorescence of fluorophore **11**, arrays were also generated using only data from fluorophores **9** and **10** (Fig. 8B and 8D). Interestingly, these arrays led to 88% differentiation between analytes. These arrays are visually different than the arrays generated using fluorophores **9-11** as predictors. There is more clustering between analytes, indicating poor separation between structurally similar analytes. This indicates that although the changes in fluorescence emission of fluorophore **11** upon analyte addition are minimal, they add more information and enable effective separation between structurally similar analytes.

Table 5 Fluorescence modulation values for analytes **1-8** with fluorophore **11**^a

Analyte	Buffer	Urine
1	1.06 ± 0.00	1.08 ± 0.00
2	1.08 ± 0.01	1.08 ± 0.01
3	1.07 ± 0.01	1.08 ± 0.00
4	1.07 ± 0.002	1.08 ± 0.00
5	1.07 ± 0.003	1.07 ± 0.00
6	1.07 ± 0.003	1.05 ± 0.01
7	1.09 ± 0.004	1.08 ± 0.01
8	1.09 ± 0.01	1.08 ± 0.00

^aAll results represent an average of results from four trials for each sample. Fluorescence modulation values were calculated using Eq. 1.

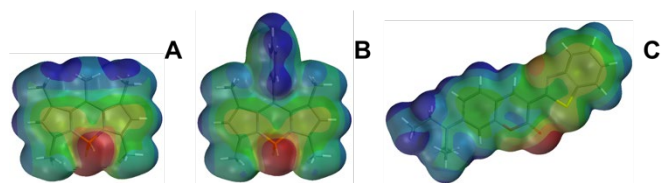


Fig. 7 Electrostatic potential maps of (A) fluorophore **9**, (B) fluorophore **10**, and (C) fluorophore **11**. All surfaces were generated using energy minimized geometries.

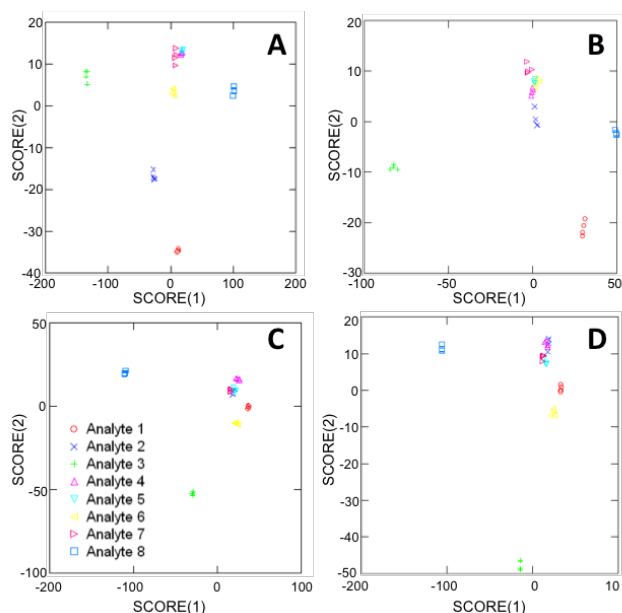


Fig. 8 Array-based detection of analytes **1-8** in (A) buffer with fluorophores **9-11** as predictors; (B) buffer with fluorophores **9** and **10** as predictors; (C) urine with fluorophores **9-11** as predictors; and (D) urine with fluorophores **9** and **10** as predictors.

In complex samples, such as human urine, it is likely multiple bisphenol analogues will be present in the event of an exposure event, or from cumulative exposure to bisphenol-containing consumer products. To address this issue, we tested the ability of our array-based detection system to differentiate between binary mixtures of bisphenol analytes (Fig. 9). Interestingly, analyte mixtures grouped on one side of the array, and samples containing one single analyte grouped on the other side of the array. This array corresponded to 100% differentiation between analyte mixtures and single analytes. Current work in our laboratory is focused on expanding these studies to include ternary and quaternary mixtures of analytes as well as different ratios of analytes in each mixture.

Limit of Detection

In addition to the ability to selectively differentiate between structurally similar analytes, it is important to be able to detect these compounds at low levels. The sensitivity of the system was determined by calculating limits of detection for all samples with fluorophore **9** following literature-reported procedures.

Fluorophore **9** was chosen for these experiments because interactions with fluorophore **9** led to the highest degree of fluorescence modulation therefore indicating extremely sensitive detection. The results of these studies are summarized in Table 6.

In general, the limits of detection for analytes in urine were slightly higher than those measured in purified buffer solutions. This is likely a result of the higher innate levels of nonpolar molecules that may compete with analytes for binding in the cyclodextrin cavity. These interactions can interfere with favourable intermolecular interactions and slightly lower the system sensitivity. While our low

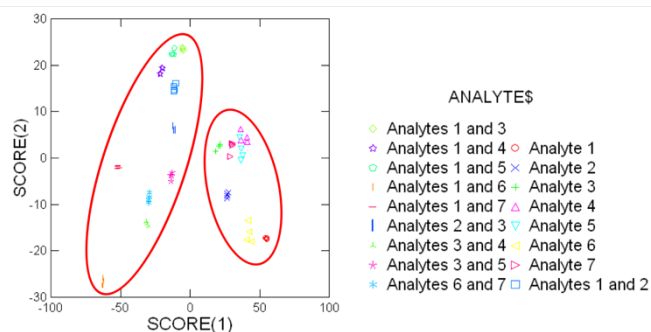


Fig. 9 Array-based detection of binary mixtures of analytes in urine using fluorophores **9-11** as predictors

Table 6 LODs for analytes **1-7** with fluorophore **9** in buffer and urine^a

Analyte	LOD in Buffer (ppm)	LOD in Urine (ppm)
1	1.51 ± 0.05	1.82 ± 0.03
2	0.14 ± 0.00	2.30 ± 0.03
3	0.01 ± 0.00	0.40 ± 0.01
4	0.29 ± 0.00	0.57 ± 0.00
5	0.39 ± 0.01	0.84 ± 0.01
6	0.49 ± 0.02	2.80 ± 0.04
7	0.39 ± 0.01	0.28 ± 0.01

^aLODs were calculated using the procedures.⁴⁰ See Electronic Supporting Information for full details.

part-per-million range detection limits show promise for the use of this detection system in other complex environments, the concentration of bisphenol compounds found in urine is in the part-per-billion range.⁵⁵ Current efforts in our laboratory are focused on lowering detection limits for cases where the detection limits are above the literature-reported exposure limits by looking at other cyclodextrin-fluorophore combinations, and/or employing a preconcentration step to achieve optimal sensitivities.

Conclusions

In summary, cyclodextrin-promoted fluorescence modulation can be used for the detection of BPA and its derivatives in both buffer and urine environments. This method is sensitive (low micromolar detection limits), selective (able to differentiate between structurally similar analytes), and broadly applicable (success in detecting analytes in buffer and complex urine environments). Future work in

our laboratory is focused on translating this highly sensitive and selective bisphenol detection method into a practical, solid-state detection device for the facile, at-home detection of BPA and derivatives in contaminated aqueous samples.

Conflicts of interest

The authors declare no conflict of interest.

Acknowledgements

Funding is acknowledged from the University of Rhode Island start-up funds and the University of Rhode Island Project Completion Grant.

Notes and references

- A. Usman and M. Ahmad, *Chemosphere*, 2016, **158**, 131.
- J. R. Rochester and A. L. Bolden, *Environ. Health Perspectives*, 2015, **123**, 643.
- A. Mantovani, *Hormone Res. Pediatrics*, 2016, **86**, 279; B. S. Ye, A. O. W. Leung and M. H. Wong, *Environ. Pollution*, 2017, **227**, 234; L. Hermabessiere, A. Dehaut, I. Paul-Pont, C. Lacroix, R. Jezequel, P. Soudant and G. Duflos, *Chemosphere*, 2017, **182**, 781.
- J. M. Braun, *Nature Rev. Endocrinology*, 2017, **13**, 161.
- A. Zhou, H. Chang, W. Huo, B. Zhang, J. Hu, W. Xia, Z. Chen, C. Xiong, Y. Zhang, Y. Wang, S. Xu, and Y. Li, *Pediatric Res.*, 2017, **81**, 851; M.-Y. Xie, H. Ni, D.-S. Zhao, L.-Y. Wen, K.-S. Li, H.-H. Yang, S.-S. Wang, H. Zhang and H. Su, *Reproductive Toxicol.*, 2016, **65**, 224.
- P. S. de Silva, X. Yang, J. R. Korzenik, R. H. Goldman, K. L. Arheart and A. J. Caban-Martinez, *Environ. Pollution*, 2017, **229**, 621.
- D. P. Provisiero, C. Pivonello, G. Muscogiuri, M. Negri, C. de Angelis, C. Simeoli, R. Pivonello and A. Colao, *Int. J. Environ. Res. Public Health*, 2016, **13**, 989/1.
- L. Del Pup, A. Mantovani, A. Luce, C. Cavaliere, G. Facchini, R. Di Francia, M. Caraglia and M. Berretta, *Oncology Rep.*, 2015, **34**, 3; M. Di Donato, G. Cerneria, P. Giovannelli, G. Galasso, A. Bilancio, A. Migliaccio and G. Castoria, *Molec. Cellular Endocrinology*, 2017, **457**, 35.
- A. Guart, F. Bono-Blay, A. Borrell and S. Lacorte, *Food Additives & Contaminants A*, 2011, **28**, 676.
- C. Z. Yang, S. I. Yaniger, V. C. Jordan, D. J. Klein and G. D. Bittner, *Environ. Health Perspectives*, 2011, **119**, 989.
- N. Poovarodom, T. Jinkarn, P. Tangmongkollert, W. Chaloeijitkul and S. Charubhum, *Packaging Technol. Sci.*, 2017, **30**, 317.
- Z. A. Moghadam, M. Mirlohi, H. Pourzamani, A. Malekpour, Z. Amininoor and M. R. Merasi, *Toxicol. Rep.*, 2015, **2**, 1273.
- L. Trasande, *Health Affairs*, 2014, **33**, 316.
- M. Eckardt, and T. J. Simat, *Chemosphere*, 2017, **186**, 1016.
- <http://eur-lex.europa.eu/legal-content/EN/TXT/?qid=1476450084033&uri=CELEX:32011L0008>;
- <http://www.washingtonpost.com/wp-dyn/content/article/2008/04/18/AR2008041803036.html>
- A. L. Brody, *Food Technol.*, 2013, **67**, 75.
- D. Milanowski, P. Pomastowski, T. Ligor, and B. Buszewski, *Critical Rev. Anal. Chem.* 2017, **47**, 251.
- S. Eladak, T. Grisin, D. Moison, M.-J. Guerquin, T. N'Tumba-Byn, S. Pozzi-Gaudin, A. Benachi, G. Livera, V. Rouiller-Fabre and R. Habert, *Fertility and Sterility*, 2015, **103**, 11.
- Z. A. Moghadam, H. Pourzamani, A. Malekpour, M. Mirlohi and Z. Amininoor, *Int. J. Environ. Health Engineering*, 2013, **2**, 1.
- M. Milanowski, P. Pomastowski, T. Ligor, and B. Buszewski, *Critical Rev. Anal. Chem.* 2017, **47**, 251.
- A. M. Calafat, X. Ye, L. Y. Wong, J. A. Reidy, and L. L. Needham, *Environ. Health Perspect.* 2008, **116**, 39.
- C. Simoneau, L. Van den Eede and S. Valzacchi, *Food Additives Contaminants A*, 2012, **29**, 469.
- H. K. Okoro, J. O. Ige, O. A. Iyiola, S. Pandey, I. A. Lawal, C. Zvinowanda and C. J. Ngila, *Fresenius Environ. Bull.*, 2017, **26**, 4623.
- R. A. Perez, B. Albergo, M. Ferriz, and J. L. Tadeo, *Anal. Bioanal. Chem.*, 2017, **409**, 4571.
- H. Wang, L. Liu, S. A. M. A. S. Eqani and H. Shen, *Anal. Sci.*, 2017, **33**, 777.
- F. Sun, L. Kang, X. Xiang, H. Li, X. Luo, R. Luo, C. Lu and X. Peng, *Anal. Bioanal. Chem.*, 2016, **408**, 6913.
- S. Guney and O. Guney, *Electroanal.* 2017, **29**, 2579.
- S. Khalililaghbab, S. Momeni, M. Farrokhnia, I. Nabipour and S. Karimi, *Anal. Bioanal. Chem.*, 2017, **409**, 2847.
- H. L. Marks, M. V. Pishko, G. W. Jackson and G. L. Cote, *Anal. Chem.*, 2014, **86**, 11614.

- ³⁰ N. Serio, D. F. Moyano, V. M. Rotello and M. Levine, *Chem. Commun.*, 2015, **51**, 11615.
- ³¹ D. J. DiScenza and M. Levine, *Supramol. Chem.*, 2016, **28**, 881; D. J. DiScenza and M. Levine, *New J. Chem.*, 2016, **40**, 789.
- ³² N. Serio, C. Chanthalya, L. Prignano and M. Levine, *Supramol. Chem.*, 2014, **26**, 714.
- ³³ D. J. DiScenza, J. Lynch, M. Verderame, N. Serio, L. Prignano, L. Gareau and M. Levine, *Supramol. Chem.*, 2018, **30**, 267.
- ³⁴ D. J. DiScenza, L. Gareau, N. Serio, J. Roque, L. Prignano, M. Verderame and M. Levine, *Anal. Chem. Lett.*, 2016, **6**, 345.
- ³⁵ N. Serio and M. Levine, *Marine Pollution Bull.*, 2015, **95**, 242; N. Serio, C. Chanthalya, L. Prignano and M. Levine, *ACS Appl. Mater. Interfaces*, 2013, **5**, 11951.
- ³⁶ N. Serio, L. Prignano, S. Peters and M. Levine, *Polycyclic Aromatic Compounds*, 2014, **34**, 561.
- ³⁷ N. Serio, K. Miller and M. Levine, *Chem. Commun.*, 2013, **49**, 4821.
- ³⁸ N. Serio, J. Roque, A. Badwal and M. Levine, *Analyst*, 2015, **140**, 7503.
- ³⁹ Y. M. Park, H. Pyo, S. J. Park, and S. K. Park, *Anal. Chim. Acta*. 2005, **548**, 109.
- ⁴⁰ D. Cheng, W. Zhao, H. Yang, Z. Huang, X. Liu, and A. Han, *Tetrahedron Lett.* 2016, **57**, 2655.
- ⁴¹ H. Tomiyasu, J. L. Zhao, X. L. Ni, X. Zeng, M. R. J. Elsegood, B. Jones, C. Redshaw, S. J. Teat, and T. Yamato, *RSC Advances* 2015, **5**, 14747.
- ⁴² S. C. Gates, C. C. Sweeley, W. Krivit, D. DeWitt, and B. E. Blaisdell, *Clin. Chem.* 1978, **24**, 1680.
- ⁴³ F. Zhang, J. Zhang, C. Tong, Y. Chen, S. Zhuang, and W. Liu, *J. Haz. Mat.* 2013, **263**, 618.
- ⁴⁴ J. A. Ruszkiewicz, A. Pinkas, B. Ferrer, T. V. Peres, A. Tsatsakis, and M. Aschner, *Toxicol. Rep.* 2017, **4**, 245.
- ⁴⁵ S. E. Schram, L. A. Glesne, and E. M. Warshaw, *Dermatitis* 2007, **18**, 221.
- ⁴⁶ T. Yuzawa, C. Watanabe, R. R. Freeman, and S. Tsuge, *Anal. Sci.* 2009, **25**, 1057.
- ⁴⁷ C. A. Staples, R. Guinn, K. Kramarz, and M. Lampi, *Human Ecol. Risk Assess.* 2011, **17**, 1057.
- ⁴⁸ C. M. Wilcox, B. Cryer and G. Triadafilopoulos, *J. Rheumatol.* 2005, **32**, 2218.
- ⁴⁹ T. Loftsson, P. Jarho, M. Masson, and T. Jarvinen, *Expert Opin. Drug Deliv.* 2005, **2**, 335.
- ⁵⁰ E. M. Martin Del Valle, *Process Biochem.* 2004, **39**, 1033.
- ⁵¹ A. A. Abdel-Shafi, M.A. Ismail and S. S. Al-Shihry, *J. Photochem. Photobiol. A: Chem.*, 2016, **316**, 52.
- ⁵² D. J. DiScenza, E. Culton, M. Verderame, J. Lynch, N. Serio, and M. Levine, *Chemosensors* 2017, **5**, 34.
- ⁵³ J. Murray, K. Kim, T. Ogoshi, W. Yao and B. C. Gibb, *Chem. Soc. Rev.*, 2017, **46**, 2479; H.-J. Schneider, F. Eblinger, J. Sartorius and J. Rammo, *J. Molec. Recognition*, 1996, **9**, 123.
- ⁵⁴ W. E. Moerner and D. P. Fromm, *Rev. Sci. Instrum.*, 2003, **74**, 3597.
- ⁵⁵ S. J. Genuis, S. Beesoon, D. Birkholz, and R. A. Lobo *J. Environ. Public Health*, 2012, **2012**, 1-10.